

RESEARCH ARTICLE



OPEN ACCESS

Received: 17.02.2021

Accepted: 13.05.2021

Published: 26.05.2021

Citation: Srikantamurthy JS, Annigeri AR (2021) Free Vibration Analysis of Multiphase Magneto-Electro-Elastic Composite Conical Shells. Indian Journal of Science and Technology 14(19): 1525-1533. <https://doi.org/10.17485/IJST/V14I18.304>

* **Corresponding author.**

Tel: 9886379067

jssmurthy@gmail.com

Funding: None

Competing Interests: None

Copyright: © 2021 Srikantamurthy & Annigeri. This is an open access article distributed under the terms of the [Creative Commons Attribution License](https://creativecommons.org/licenses/by/4.0/), which permits unrestricted use, distribution, and reproduction in any medium, provided the original author and source are credited.

Published By Indian Society for Education and Environment ([iSee](https://www.indst.org/))

ISSN

Print: 0974-6846

Electronic: 0974-5645

Free Vibration Analysis of Multiphase Magneto-Electro-Elastic Composite Conical Shells

J S Srikantamurthy^{1*}, Anandkumar R Annigeri¹

¹ Department of Mechanical Engineering, JSS Academy of Technical Education, Affiliated to Visvesvaraya Technological University, Belagavi, Karnataka, Bangalore, 560060, India. Tel.: 9886379067

Abstract

Objectives: In the present article, free vibration of multiphase Magneto-Electro-Elastic (MEE) conical shell having a uniform thickness is examined for Clamped-Free (C-F) boundary condition. **Method:** The study is carried out using a semi-analytical approach for different volume fractions (V_f) 0, 0.2, 0.6 and 1.0 of BaTiO₃ in BaTiO₃-CoFe₂O₄ smart composite conical shell for three different semi-vertex angles 20°, 35° and 50°. The piezoelectric (P_e) and piezomagnetic (P_m) phase on natural frequencies of MEE truncated conical shells are discussed for different circumferential modes. **Findings:** The parametric study indicates that natural frequency decrease with an increase in V_f of BaTiO₃ in magneto-electro-elastic truncated conical shells. **Novelty:** Studies on MEE constant thickness truncated conical shell using BaTiO₃ and CoFe₂O₄ as (P_e) & (P_m) smart composite for clamped-free boundary condition to analyse the effect of the frequency with different semi-vertex angle and cone heights. Present commercial FEA software tools are limited to 2 coupling fields. In this research, coupling between 3 fields considered for MEE material. Hence, a computer code is developed to study the influence coupling between electric, elastic and magnetic fields, which can be used for any combinations of boundary conditions and volume fractions.

Keywords: MagnetoElectroElastic (MEE); axisymmetric constant thickness conical shell; Smart Composites; volume fraction; free vibrations; finite element method

1 Introduction

Smart materials and smart structures are important as they have wide varieties of applications in engineering such as sensors, actuators and especially in vibration and noise control. Several materials and technologies have been proposed and investigated. Axisymmetric conical shells are shown their applications in aerospace and shipbuilding. A numerical approach is used to obtain the frequency for conical shell for different boundary conditions⁽¹⁾. The vibration behaviour of the axisymmetric conical shell was analysed using FEM and optimization studies were carried out⁽²⁾. A study is conducted for the vibration of the conical shell having different cone angles with constant and

varying thickness⁽³⁾. The frequency characteristics of the truncated conical shell are studied having different geometric parameters⁽⁴⁾. Free vibration of MEE cylindrical shell analysed using governing equations⁽⁵⁾. kernel particle (kp) functions are used to study the thin conical shell⁽⁶⁾. A study is conducted to know the piezomagnetic effect on multiphase MEE cylindrical shell⁽⁷⁾. Shell and plates behaviour is analysed using the differential quadrature method⁽⁸⁾. Novozhilov theory is used to investigate thick cones with smaller height for different vertex angles and end conditions⁽⁹⁾. The study is conducted on the conical shell using closed-form auxiliary functions along with the Rayleigh-Ritz procedure⁽¹⁰⁾. The truncated composite conical shell is analysed for different volume fraction using third-order shear deformation theory⁽¹¹⁾. A study is conducted on free vibration conical shell using FSDT with six degrees of freedom in the direction of thickness⁽¹²⁾. Conical shell is analysed using Flügge thin shell theory with different boundary conditions⁽¹³⁾. Multi-layered conical shell analysed using coupled differential equations and spline approximation method⁽¹⁴⁾. Truncated conical shell behaviour studied using arbitrary boundary conditions employing Hamilton's principle⁽¹⁵⁾. Free vibration of MEE plates analysed using condensation technique⁽¹⁶⁾. Magneto-Electro-Elastic plates studied using the Hamilton's principle⁽¹⁷⁾. Review is made on different techniques to analyse the behaviour of MEE materials.⁽¹⁸⁾ Research on conical shell vibration under various parameters effect like boundary conditions, cone angle, thickness, radius to height ratio, length to radius ratio has attracted attention in engineering^(19,20).

With the literature view, numerous works are carried out of free vibration on the conical shell using standard numerical methods. Meanwhile, a very less study on MEE truncated conical shell using BaTiO₃ and CoFe₂O₄ as (P_e) & (P_m) smart composite for clamped-free boundary condition. At present, a parametric study has been performed to analyse the effect of the frequency with different semi-vertex angle and cone heights.

2 Formulation

The governing equations of MEE are referred for deriving the FE model in r, θ, z coordinate system such that material properties and geometry remains same in 'q' direction^{(5) (7)}.

Free vibration studies for different V_f of MEE conical shell is conducted for Clamped-Free boundary condition. The conical shell structure is modelled using three noded triangular elements with three degrees of freedom (DOF) for each node.

The equations used in the finite element model are;

$$S_r = S_1 = \frac{\partial u_r}{\partial r}; S_\theta = S_2 = \frac{1}{r} \left(\frac{\partial u_\theta}{\partial \theta} + u_r \right); S_z = S_3 = \frac{\partial u_z}{\partial z}; \gamma_{zr} = \frac{\partial u_z}{\partial r} + \frac{\partial u_r}{\partial z} \quad (1)$$

Where u_r, u_θ and u_z are mechanical displacements.

The relation between electric field vector (E) & electric potential (ϕ) is.

$$E_r = E_1 = -\frac{\partial \phi}{\partial r}; E_z = E_3 = -\frac{\partial \phi}{\partial z} \quad (2)$$

The relation between magnetic field (H) & magnetic potential (ψ) is.

$$H_r = H_1 = -\frac{\partial \psi}{\partial r}; H_z = H_3 = -\frac{\partial \psi}{\partial z} \quad (3)$$

Equation (4) shows a coupled linear MEE material matrix, for axi-symmetric conical shell having planes of symmetry in axial direction^{(5) (7)}.

$$\begin{Bmatrix} \sigma_r \\ \sigma_\theta \\ \sigma_z \\ \tau_{zr} \\ D_r \\ D_z \\ B_r \\ B_z \end{Bmatrix} = \begin{bmatrix} C_{11} & C_{12} & C_{13} & 0 & 0 & e_{31} & 0 & q_{31} \\ C_{12} & C_{11} & C_{13} & 0 & 0 & e_{31} & 0 & q_{31} \\ C_{13} & C_{13} & C_{33} & 0 & 0 & e_{33} & 0 & q_{33} \\ 0 & 0 & 0 & C_{44} & e_{15} & 0 & q_{15} & 0 \\ 0 & 0 & 0 & e_{15} & \epsilon_{11} & 0 & m_{11} & 0 \\ e_{31} & e_{31} & e_{33} & 0 & 0 & \epsilon_{33} & 0 & m_{33} \\ 0 & 0 & 0 & q_{15} & m_{11} & 0 & \mu_{11} & 0 \\ q_{31} & q_{31} & q_{33} & 0 & 0 & m_{33} & 0 & \mu_{33} \end{bmatrix} \begin{Bmatrix} S_r \\ S_\theta \\ S_z \\ \gamma_{zr} \\ E_r \\ E_z \\ H_r \\ H_z \end{Bmatrix} \quad (4)$$

$\sigma_r, \sigma_\theta, \sigma_z, \tau_{zr}$ are Stress components; D_r, D_z are electrical displacements; B_r, B_z are magnetic displacements; $\epsilon_r, \epsilon_\theta, \epsilon_z, \gamma_{zr}$ are strains; E_r, E_z indicate electric fields; H_r, H_z represents magnetic fields.

C_{ij}, ϵ_{ij} and μ_{ij} are elastic, dielectric and magnetic permeability constants and e_{ij}, q_{ij} and m_{ij} are the P_e, P_m and magneto-electric material constants respectively.

For free vibration studies⁽⁵⁾⁽⁷⁾,

$$[M]\{\ddot{u}\} + [K_{ME}]\{u\} = 0, \text{ Where} \quad (5)$$

$$[K_{MEE}] = [K_{uu}] + [K_{u\phi}] [K_B]^{-1} [K_A] + [K_{u\psi}] [K_D]^{-1} [K_C] \quad (6)$$

$[K_{MEE}]$ = Stiffness matrix for fully coupled magneto-electro-elastic material.

$[K_{uu}]$ = Structural stiffness matrix considering elastic constants

$[K_u]$ = Structural stiffness matrix considering coupled elastic – electric potential material.

The component matrices of equation

$$[K_A] = [K_{u\phi}]^T - [K_{\phi\psi}] [K_{\psi\psi}]^{-1} [K_{u\psi}]^T \quad (7)$$

$$[K_B] = [K_{\phi\phi}] - [K_{\phi\psi}] [K_{\psi\psi}]^{-1} [K_{\phi\psi}]^T \quad (8)$$

$$[K_C] = [K_{u\psi}]^T - [K_{\phi\psi}]^T [K_{\phi\phi}]^{-1} [K_{u\phi}]^T \quad (9)$$

$$[K_D] = [K_{\psi\psi}] - [K_{\phi\psi}]^T [K_{\phi\phi}]^{-1} [K_{\phi\psi}] \quad (10)$$

The distribution of $\{\phi\}$ and $\{\psi\}$ are

$$\phi = [K_B]^{-1} [K_A] \{u\} \quad (11)$$

$$\psi = [K_D]^{-1} [K_C] \{u\}$$

2.1 Volume Fraction (V_f) P_e phase in MEE Conical Shell

The analysis is conducted for V_f (0, 0.2, 0.6, and 1.0) of P_e phase in MEE smart materials. The density for MEE material is 5730 kg m^{-3} ⁽⁷⁾.

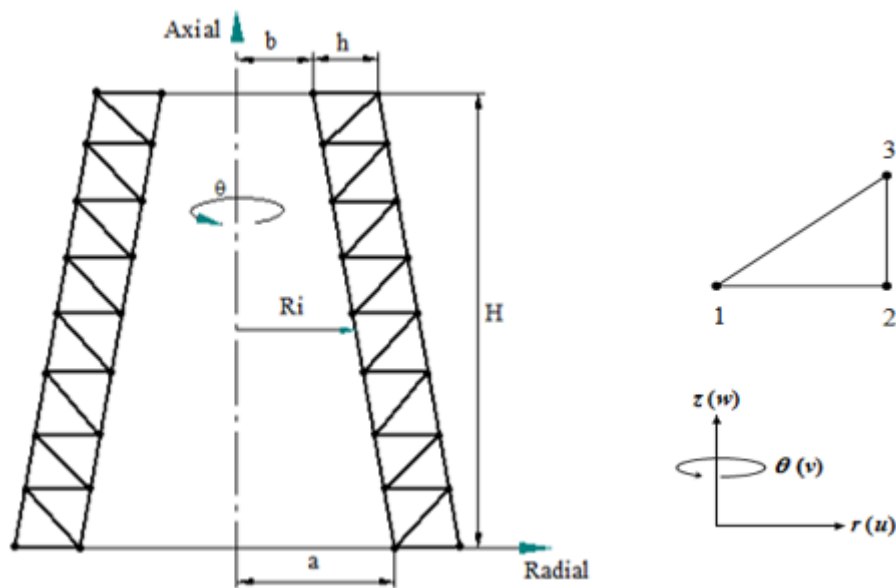


Fig 1. FEM Discretization of MEE conical shell using triangular elements

Figure 1 shows the geometry of the axisymmetric MEE conical shell, where h is the thickness of the cone, a is the larger base & b is the small base of the cone. H is the cone height & α is the semi-vertex angle. R_i represents the distance of the internal surface from the central axis.

3 Geometric and Material Modeling

Free vibration studies of the conical shell are conducted by varying semi vertex cone angle (α), cone height (H) with a constant thickness (h), base radius (a) and top radius (b). The dimensions of the MEE conical shell used in the study are base radius (a=1m), top radius (b=0.5m), constant thickness (h=0.1m) for three values of semi vertex angle ($\alpha = 20^\circ$, $\alpha = 35^\circ$ and $\alpha = 50^\circ$). The numbers of triangular finite elements in radial and axial directions are selected as in Table 1, for a better aspect ratio.

Table 1. Elements for semi vertex angle (α)

Sl. No.	Semi vertex angle	Elements in Radial direction	Elements in Axial direction	Total Number of Elements
1	20°	4	56	448
2	35°	5	42	420
3	50°	7	40	560

The notations used are: ω_{uu} = Frequency in rad/sec by using $[K_{uu}]$, ω_{MEE} = Frequency in rad/sec by using $[KMEE]$

Table 2. Material coefficients of BaTiO₃-CoFe₂O₄ composite^{(5) (7)}

V_f	0	0.2	0.6	1.0
C_{11}	286×10^9	250×10^9	200×10^9	166×10^9
C_{12}	173×10^9	146×10^9	110×10^9	77×10^9
C_{13}	170×10^9	145×10^9	110×10^9	78×10^9
C_{33}	269.5×10^9	240×10^9	190×10^9	162×10^9
C_{44}	45.3×10^9	45×10^9	45×10^9	43×10^9
e_{31}	0	-2	-3.5	-4.4
e_{33}	0	4	11	18.6
e_{15}	0	0	0	11.6
e_{11}	0.08×10^{-9}	0.33×10^{-9}	0.9×10^{-9}	11.2×10^{-9}
e_{33}	0.093×10^{-9}	2.5×10^{-9}	7.5×10^{-9}	12.6×10^{-9}
m_{11}	-5.9×10^{-4}	-3.9×10^{-4}	-1.5×10^{-4}	0.05×10^{-4}
m_{33}	1.57×10^{-4}	1.33×10^{-4}	0.75×10^{-4}	0.1×10^{-4}
q_{31}	580	410	200	0
q_{33}	700	550	260	0
q_{15}	560	340	180	0
m_{11}	0	2.8×10^{-12}	6.0×10^{-12}	0
m_{33}	0	2000×10^{-12}	2500×10^{-12}	0

Here C_{ij} in N/m², e_{ij} in C/m², e_{ij} in C/Vm, q_{ij} in N/A m, m_{ij} in N s²/C² & m_{ij} in N s/VC.

4 Results & Discussion

The axisymmetric finite element code developed is tested for different boundary conditions and is validated with the published literature. The results of the validation are discussed in section 4.1 and analysis of Clamped-Free boundary condition of MEE conical shells for three semi vertex angle $\alpha = 20^\circ$, $\alpha = 35^\circ$, $\alpha = 50^\circ$ and V_f studies from 0 to 1.0 are shown in section 4.2.

4.1 Validation

The developed computer code for MEE conical shell finite element analysis is validated⁽³⁾ and the results of the validation show good agreement. The dimensions of the isotropic conical shell are $R/H = 0.3$, base radius ($R = 1.25$ m), constant thickness ($h = 0.0625$ m), density is 2410 kg m^{-3} , Young's modulus ($E = 30 \times 10^9 \text{ Nm}^{-2}$).

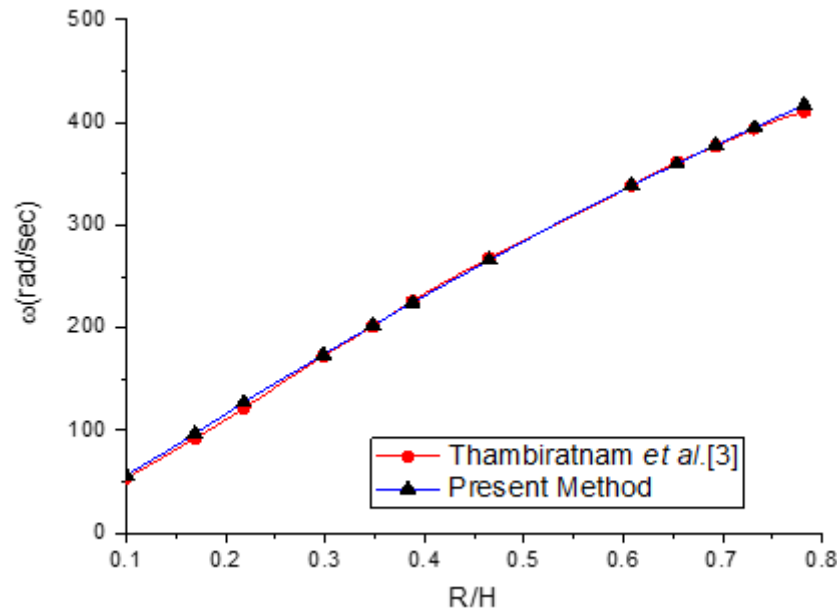


Fig 2. Plots of Frequency for different R/H (base radius/cone height) ratio

4.2 Analysis of MEE conical shell for Clamped-Free boundary condition

Here free vibration studies on three MEE conical shells with different semi vertex angle, viz., $\alpha=20^\circ$, $\alpha=35^\circ$ and $\alpha=50^\circ$ are conducted for constant V_f of 0,0.2,0.6 and 1.0 BaTiO₃ in MEE composite is chosen. The two end conditions of the MEE shell study are Clamped-Free (E-F) viz.,

(i) The top end is clamped with a bottom end is free ($u = v = w = \phi = \psi = 0$, at $z = H$).

(ii) The top end is free with the bottom end is clamped ($u = v = w = \phi = \psi = 0$, at $z = 0$)

4.2.1 Analysis of MEE conical shell for $V_f = 0$

The study conducted on Clamped-Free boundary condition for $V_f = 0$ and Tables 3 and 4 shows the results of the study. Table 3 shows the frequency for top-end clamped and bottom end free conical shell and Table 4 shows results for top-end free and bottom end clamped. The frequency value in Table 4 is predominantly high compared with the frequency in Table 3, which indicates that with an increase in semi vertex angle, the frequency of the shell increases. An influence of coupling effect is observed in free vibrations of ω_{MEE} compared to ω_{uu} for all the three $\alpha=20^\circ$, $\alpha=35^\circ$ and $\alpha=50^\circ$ semi vertex angles.

Table 3. Top end fixed with bottom end free condition

Semi vertex angle	$\alpha = 20^\circ$		$\alpha = 35^\circ$		$\alpha = 50^\circ$	
Frequency (rad/sec)	ω_{vv}	ω_{MEE}	ω_{vv}	ω_{MEE}	ω_{vv}	ω_{MEE}
1	1255	1253	2041	2038	2218	2214
2	868.7	866.9	1432	1427	1655	1650
3	1387	1386	1564	1561	1640	1635
4	2400	2398	2313	2311	2102	2099
5	3686	3684	3423	3422	2913	2911
6	5199	5195	4770	4769	3963	3961
7	6909	6905	6305	6302	5190	5189
8	8794	8788	7997	7995	6562	6561
9	10830	10820	9828	9825	8056	8054
10	13000	12990	11780	11770	9653	9651

Table 4. Top end free with bottom end fixed condition

Semi vertex angle	$\alpha = 20^0$		$\alpha = 35^0$		$\alpha = 50^0$	
Frequency (rad/sec)	ω_{uu}	ω_{MEE}	ω_{uu}	ω_{MEE}	ω_{uu}	ω_{MEE}
1	2703	2702	4229	4226	4321	4316
2	1832	1830	2936	2930	3332	3327
3	2829	2826	3324	3316	3453	3446
4	4323	4317	4817	4805	4586	4576
5	6027	6019	6654	6636	6203	6188
6	7947	7937	8652	8628	8057	8035
7	10050	10040	10790	10760	10060	10030
8	12320	12310	13050	13010	12180	12150
9	14720	14710	15420	15390	14400	14360
10	17240	17230	17900	17860	16710	16670

4.2.2 Analysis of MEE conical shell for $V_f = 0.2$

The study conducted on Clamped-Free boundary condition for $V_f = 0.2$ and Tables 5 and 6 shows the results of the study. Table 5 shows the frequency for top-end clamped and bottom end free conical shell and Table 6 shows results for top-end free and bottom end clamped. As the semi-vertex angle increases the frequency values in Table 5 is low compared with the frequency values in Table 6.

Table 5. Top end fixed with bottom end free condition

Semi vertex angle	$\alpha = 20^0$		$\alpha = 35^0$		$\alpha = 50^0$	
Frequency (rad/sec)	ω_{uu}	ω_{MEE}	ω_{uu}	ω_{MEE}	ω_{uu}	ω_{MEE}
1	1236	1242	1999	2003	2156	2158
2	844.2	851.4	1400	1402	1615	1613
3	1334	1341	1517	1522	1596	1595
4	2305	2315	2230	2241	2033	2038
5	3540	3555	3294	3311	2807	2818
6	4991	5012	4588	4612	3813	3830
7	6632	6660	6062	6094	4991	5015
8	8441	8476	7690	7730	6310	6341
9	10400	10440	9451	9500	7747	7785
10	12480	12530	11330	11390	9286	9331

Table 6. Top end free with bottom end fixed condition

Semi vertex angle	$\alpha = 20^0$		$\alpha = 35^0$		$\alpha = 50^0$	
Frequency (rad/sec)	ω_{uu}	ω_{MEE}	ω_{uu}	ω_{MEE}	ω_{uu}	ω_{MEE}
1	2667	2677	4131	4140	4178	4188
2	1787	1796	2875	2876	3241	3242
3	2723	2727	3222	3225	3350	3353
4	4158	4161	4644	4650	4429	4439
5	5793	5796	6412	6418	5981	5997
6	7633	7637	8338	8345	7767	7788
7	9652	9658	10390	10400	9703	9728
8	11820	11830	12570	12580	11750	11780
9	14130	14140	14850	14880	13890	13930
10	16550	16560	17240	17270	16120	16160

4.2.3 Analysis of MEE conical shell for $V_f = 0.6$

The study conducted on C-F boundary condition for $V_f = 0.6$ and Tables 7 and 8 shows the results of the study. Table 7 shows the frequency for top-end clamped and bottom end free conical shell and Table 8 shows results for top-end free and bottom end clamped. In Table 7, the frequency value in Table 8 is largely high compared with the frequency values in Table 7, indicating that as semi vertex angle increases the frequency also increases due to the stiffening of the conical shell, similar behaviour is observed in coupled frequency.

Table 7. Top end fixed with bottom end free condition

Semi vertex angle	$\alpha = 20^0$		$\alpha = 35^0$		$\alpha = 50^0$	
Frequency (rad/sec)	ω_{uu}	ω_{MEE}	ω_{uu}	ω_{MEE}	ω_{uu}	ω_{MEE}
1	1198	1216	1926	1937	2051	2046
2	797.4	816.4	1344	1352	1548	1532
3	1244	1258	1436	1449	1523	1512
4	2149	2167	2091	2112	1919	1920
5	3300	3325	3080	3110	2631	2645
6	4652	4686	4285	4326	3563	3589
7	6181	6224	5661	5714	4659	4696
8	7865	7920	7181	7248	5889	5937
9	9688	9754	8827	8910	7231	7291
10	11630	11710	10580	10680	8671	8743

Table 8. Top end free with bottom end fixed condition

Semi vertex angle	$\alpha = 20^0$		$\alpha = 35^0$		$\alpha = 50^0$	
Frequency (rad/sec)	ω_{uu}	ω_{MEE}	ω_{uu}	ω_{MEE}	ω_{uu}	ω_{MEE}
1	2601	2629	3963	3982	3935	3939
2	1706	1731	2773	2779	3086	3070
3	2549	2560	3056	3062	3180	3159
4	3887	3898	4361	4371	4168	4153
5	5409	5422	6012	6023	5611	5594
6	7120	7136	7819	7832	7283	7261
7	8998	9016	9746	9765	9101	9077
8	11020	11040	11780	11810	11030	11010
9	13160	13190	13920	13960	13040	13030
10	15420	15440	16150	16200	15130	15130

4.2.4 Analysis of MEE conical shell for $V_f = 1$

The study conducted on C-F boundary condition for $V_f = 1$ and Tables 9 and 10 shows the results of the study. Table 9 shows the frequency for top-end clamped and bottom end free conical shell and Table 10 shows results for top-end free and bottom end clamped. As the semi-vertex angle increases the frequency values in Table 9 is predominantly less compared with the frequency values in Table 10.

Table 9. Top end fixed with bottom end free condition

Semi vertex angle	$\alpha = 20^0$		$\alpha = 35^0$		$\alpha = 50^0$	
Frequency (rad/sec)	ω_{uu}	ω_{MEE}	ω_{uu}	ω_{MEE}	ω_{uu}	ω_{MEE}
1	1173	1205	1886	1918	2009	2031
2	779.2	811.1	1310	1345	1508	1526
3	1211	1227	1401	1432	1485	1504
4	2091	2105	2043	2070	1878	1898
5	3211	3229	3009	3037	2578	2602
6	4528	4551	4187	4221	3492	3523
7	6017	6046	5531	5573	4566	4605
8	7660	7695	7018	7069	5772	5820
9	9439	9481	8629	8691	7089	7147
10	11340	11390	10350	10420	8502	8571

Table 10. Top end free with bottom end fixed condition

Semi vertex angle	$\alpha = 20^0$		$\alpha = 35^0$		$\alpha = 50^0$	
Frequency (rad/sec)	ω_{uu}	ω_{MEE}	ω_{uu}	ω_{MEE}	ω_{uu}	ω_{MEE}
1	2553	2597	3883	3918	3848	3879
2	1665	1712	2709	2751	3023	3045
3	2462	2487	2965	3003	3098	3125
4	3745	3781	4214	4258	4046	4084
5	5212	5255	5800	5859	5433	5486
6	6865	6912	7543	7615	7041	7110
7	8682	8733	9407	9490	8794	8879
8	10640	10700	11380	11470	10660	10760
9	12720	12780	13460	13560	12610	12720
10	14910	14970	15630	15740	14640	14770

5 Conclusions

- In the C-F boundary condition, the influence of the coupling effect is observed in free vibrations of ω_{MEE} compared to ω_{uu} for different semi vertex angles.
- For the $V_f = 0$ and $V_f = 1$, the 'm' effect influence is not predominant.
- Irrespective of V_f and semi vertex angle, it is clearly said that when the truncated conical shell bottom is clamped and the top is free, the average piezoelectric and piezomagnetic effect is high around 54 percent compared to the condition when the bottom end is free and the top end is clamped.
- The effect of clamping the bottom end and clamping the top end is seen in the study as the conical shell becomes stiffer.
- The effect of P_e and P_m are prominent at initial circumferential modes while it is negligible at higher circumferential modes.

References

- 1) Irie T, Yamada G, Kaneko Y. Natural frequencies of truncated conical shells. *Journal of Sound and Vibration*. 1984;92(3):447–453. Available from: [https://doi.org/10.1016/0022-460X\(84\)90391-2](https://doi.org/10.1016/0022-460X(84)90391-2).
- 2) Thambiratnam DP, Thevendran V. Optimum design of conical shells for free vibration. *Computers & Structures*. 1988;29(1):133–140. Available from: [https://dx.doi.org/10.1016/0045-7949\(88\)90178-2](https://dx.doi.org/10.1016/0045-7949(88)90178-2).
- 3) Thambiratnam PD, Zhuge Y. Axisymmetric free vibration analysis of conical shells. *Engineering Structure*. 1991;15(2). Available from: [https://doi.org/10.1016/0141-0296\(93\)90002-L](https://doi.org/10.1016/0141-0296(93)90002-L).
- 4) Lam KY, Hua L. Vibration analysis of a rotating truncated circular conical shell. *International Journal of Solids and Structures*. 1997;34(17):2183–2197. Available from: [https://dx.doi.org/10.1016/S0020-7683\(96\)00100-X](https://dx.doi.org/10.1016/S0020-7683(96)00100-X).

- 5) Buchanan GR. Free vibration of an infinite magneto-electro-elastic cylinder. *Journal of Sound and Vibration*. 2003;268:413–426. Available from: [10.1016/S0022-460X\(03\)00357-2](https://doi.org/10.1016/S0022-460X(03)00357-2).
- 6) Liew KM, Ng TY, Zhao X. Free vibration analysis of conical shells via the element-free kp-Ritz method. *Journal of Sound and Vibration*. 2005;281(3-5):627–645. Available from: <https://dx.doi.org/10.1016/j.jsv.2004.01.005>.
- 7) Annigeri AR, Ganesan N, Swarnamani S. Free vibrations of clamped–clamped magneto-electro-elastic cylindrical shells. *Journal of Sound and Vibration*. 2006;292(1-2):300–314. Available from: <https://dx.doi.org/10.1016/j.jsv.2005.07.043>.
- 8) Tornabene F, Viola E, Inman DJ. 2-D differential quadrature solution for vibration analysis of functionally graded conical, cylindrical shell and annular plate structures. *Journal of Sound and Vibration*. 2009;328(3):259–290. Available from: <https://dx.doi.org/10.1016/j.jsv.2009.07.031>.
- 9) Firouz-Abadi RD, Rahmiani M, Amabili M. Free Vibration of Moderately Thick Conical Shells Using a Higher Order Shear Deformable Theory. *Journal of Vibration and Acoustics*. 2014;136(5):1–8. Available from: <https://dx.doi.org/10.1115/1.4027862>.
- 10) Jin G, Ma X, Shi S, Ye T, Liu Z. A modified Fourier series solution for vibration analysis of truncated conical shells with general boundary conditions. *Applied Acoustics*. 2014;85:82–96. Available from: <https://dx.doi.org/10.1016/j.apacoust.2014.04.007>.
- 11) Nejati M, Asanjarani A, Dimitri R, Tornabene F. Static and free vibration analysis of functionally graded conical shells reinforced by carbon nanotubes. *International Journal of Mechanical Sciences*. 2017;130:383–398. Available from: <https://dx.doi.org/10.1016/j.ijmecsci.2017.06.024>.
- 12) Mouli BC, Kar VR, Ramji K, Rajesh M. Free vibration of functionally graded conical shell. *Materials Today: Proceedings*. 2018;5(6):14302–14308. Available from: <https://dx.doi.org/10.1016/j.matpr.2018.03.012>.
- 13) Wu C, Pang F. Free Vibration Characteristics of the Conical Shells Based on Precise Integration Transfer Matrix Method. *Latin American Journal of Solids and Structures*. 2018;15(1):e03. Available from: <http://dx.doi.org/10.1590/1679-78253971>.
- 14) Javed S. Free vibration characteristic of laminated conical shells based on higher-order shear deformation theory. *Composite Structures*. 2018;204:80–87. Available from: <https://doi.org/10.1016/j.compstruct.2018.07.065>.
- 15) Song Z, Cao Q, Dai Q. Free vibration of truncated conical shells with elastic boundary constraints and added mass. *International Journal of Mechanical Sciences*. 2019;155:286–294. Available from: <https://dx.doi.org/10.1016/j.ijmecsci.2019.02.039>.
- 16) Vinyas M, Sandeep AS, Nguyen-Thoi T, Ebrahimi F, Duc DN. A finite element–based assessment of free vibration behaviour of circular and annular magneto-electro-elastic plates using higher order shear deformation theory. *Journal of Intelligent Material Systems and Structures*. 2019;30(16):2478–2501. Available from: <https://dx.doi.org/10.1177/1045389x19862386>.
- 17) Vinyas M, Sunny KK, Harursampath D, Nguyen-Thoi T, Loja MAR. Influence of interphase on the multi-physics coupled frequency of three-phase smart magneto-electro-elastic composite plates. *Composite Structures*. 2019;226:111254. Available from: <https://dx.doi.org/10.1016/j.compstruct.2019.111254>.
- 18) Vinyas M. Computational Analysis of Smart Magneto-Electro-Elastic Materials and Structures: Review and Classification. *Archives of Computational Methods in Engineering*. 2021;28(3):1205–1248. Available from: <https://dx.doi.org/10.1007/s11831-020-09406-4>.
- 19) Leissa AW, National Aeronautics and Space Administration. Vibration of shell. 1973.
- 20) Li H. Rotating Shell Dynamics. 2005.